Fabrication of zinc-nano TiO$_2$ composite films: Electrochemical corrosion studies

M. K. Punith Kumar and T. V. Venkatesha*

Department of PG Studies & Research in Chemistry, Kuvempu University, Shankaraghatta, India
_____

ABSTRACT

The composite coating of zinc-TiO$_2$ was generated successfully on steel from the optimized zinc electroplating bath containing TiO$_2$ nanoparticles. The composite zinc-TiO$_2$ coating produced from bath solution with different amount of TiO$_2$ was tested for their corrosion behavior by electrochemical studies using polarization and Impedance methods. The TiO$_2$ incorporated zinc coatings shown better corrosion resistance towards aggressive media when compare to pure zinc coating. The surface structure was examined from their scanning electron microscopic images and X-ray diffraction spectra. The presence of TiO$_2$ in the coating was confirmed from energy dispersive X-ray diffraction spectra. The embedded TiO$_2$ nanoparticles changed the compactness, microstructure and preferred orientation of the deposit when compare to pure zinc coating.

Keywords: Zinc-TiO$_2$ composite coating, Degussa TiO$_2$, Electrodeposition, Corrosion, EIS.
_____

INTRODUCTION

Zinc deposition is used to protect the steel from corrosion because of its sacrificial nature. However, zinc itself undergoes corrosion leading to the formation of white colored products on zinc surface. This can be controlled by post plating process such as chromate passivation or surface modification with organic chelating agents. But the chromium salts and other organic agents which are used in surface modification process are toxic in nature and therefore their use is restricted [1].

The steel materials can also be protected by generating good zinc composite coating on its surface from plating bath. The generally used particles for zinc composite coatings are ceramics, polymers, metal oxides or metal carbides etc. The plating baths containing suspended or dispersed particles of sizes in micro or nano scale are used to get composite coatings. In recent years nanoparticles instead of micro particles are employed largely in composite coating because of their advantageous properties along with their easy availability [2].

In metal-nanoparticle composites coating the second phase particles are oxides, carbides or nitrides of different metals [3].

The deposit incorporated with the WC [1], ZrO$_2$ [4], WC [5], Al$_2$O$_3$ [6, 7], and SiC [8] nanoparticles shows higher wear resistance with hardness. The codeposition of Al$_2$O$_3$ [7], SiC [8], CNT [9], TiO$_2$ [10], Graphite [11] and SiO$_2$ [12] particles with metal matrix provide high corrosion resistance property to the composite. Also the incorporation of particles like MoS$_2$, graphite, PTFE in to the metal matrix exhibit more self lubrication property [12, 13]. Hence the inclusion of these nano particles leads to improvement in physical, mechanical and electrochemical properties of zinc electroplating.

The nanosized TiO$_2$ particles are in great demand for the generation of composite zinc coatings on steel because they exhibit properties like photo induced biocidal effect [14], semiconducting, photocatalytic [15, 16, 17], wear and

corrosion resistance [10]. The zinc metal matrix with TiO_2 nanoparticles predominantly shows higher corrosion resistance property due to considerable morphological changes in the deposit and it is confirmed by our previous report on the corrosion behavior of zinc-TiO_2 nanocomposite [10].

In the literature different methods were reported for generation of zinc-TiO_2 composite [10, 14, 18]. For testing their corrosion behavior always chemical and electrochemical methods were employed. The authors B.M. Praveen et. al., used polarization and weight loss method to study the corrosion behavior of zinc-TiO_2 composite coatings [10]. G.M. Treacy [19] and co-workers studied the corrosion behavior of chromate passivated alluminium alloy using electrochemical impedance method.

Many authors in their studies selected a single concentration of nanoparticles in the bath to generate composite coating and then measured its properties along with their corrosion behavior. Therefore the present study was directed to fabricate the zinc-TiO_2 composite from solutions containing different amount of TiO_2. The composite coating of zinc-TiO_2 was obtained on mild steel from the optimized bath solution containing different amount of TiO_2. The corrosion behavior of so obtained composite coating was tested by electrochemical methods. The scanning electron microscopy (SEM), X-ray diffraction (XRD) and energy dispersive X-ray diffraction (EDX) data were used to characterize the composite coating.

EXPERIMENTAL SECTION

Zinc-TiO_2 composite coatings were generated on mild steel specimen from the zinc plating bath (Table 1) containing suspended Degussa TiO_2 nanoparticles of size 35 nm. The plating solutions were prepared by adding 1, 3 and 5 g L^{-1} of Degussa TiO_2 nanoparticles and were stirred for 24 hrs by magnetic stirrer to ensure uniform dispersion of nanoparticles in plating solution. For plating process, the mild steel (AISI 1079, composition C=0.5%, Mn=0.5%, S=0.005% and Fe=98.95%) with area 4×4 cm^2 and Zn metal plate of same area were used as cathode and anode respectively.

The mild steel plates were polished mechanically and degreased with trichloroethylene in degreaser plant followed by water wash mean while the plates were dipped in 10% HCl to remove the rust and finally rinsed in water. The zinc plate was used as anode and its surface was activated by dipping in 5% HCl for few seconds followed by water wash. Equal dimension (4 cm X 4 cm) of mild steel and zinc (99.99%) plates were selected as cathode and anode for the plating process. The electrodeposition process was carried out at current density of 0.03 A cm^{-2} for 10 minutes with 300 rpm solution stirring speed at 27 ± 2 °C.

For all electrochemical measurements the CHI 660C electrochemical work station (U.S. make) was used. A conventional cell with platinum as counter, saturated calomel as reference and specimen under investigation as working electrode was used. For polarization and EIS measurements the electrolyte used was 3.5% NaCl. The morphology of coated samples studied from SEM, XRD and EDX data.

RESULTS AND DISCUSSION

Deposition of zinc and zinc-TiO_2 composite coatings.
For pure zinc deposition the steel specimen and zinc plate of area 4×4 cm^2 were used as cathode and anode respectively. The cathode surface was prepared by the procedure as mentioned in the experimental part. The deposit was obtained using optimized bath (Table 1) by applying 0.03 A cm^{-2} current for 10minutes with solution stirring speed of 300 rpm. The deposit was represented by C_0.

Table-1: Optimized bath composition and operating parameters for zinc deposition

Bath	Constituents	Concentration	Deposit code	Operating parameters
Basic	$ZnSO_4$	180 g L^{-1}	C_0	Anode: Zinc plate
bath	Na_2SO_4	30 g L^{-1}		Cathode: Mild steel plate
(BB)	NaCl	10 g L^{-1}		Current density: 0.03 A cm^{-2}
	SLS	1.5 mM		Plating time: 10 min
BT_1	Degussa TiO_2+BB	1 g L^{-1}	C_1	Stirring speed: 300 rpm
BT_2	Degussa TiO_2+BB	3 g L^{-1}	C_3	pH:2.5
BT_3	Degussa TiO_2+BB	5 g L^{-1}	C_5	Temperature: 27 ± 2 °C

Three solutions of bath (Table 1) each containing 1, 3 and 5 g L^{-1} of TiO_2 were prepared and each solution was stirred 24 hours for uniform dispersion of nanoparticles. The zinc-TiO_2 composite coatings were fabricated from

_____

these solutions under similar plating conditions mentioned above. The deposits were named in different deposit code and given in Table 1. These coatings were subjected to corrosion behavior studies and surface characterization.

Corrosion behavior of zinc and zinc-TiO$_2$ composite coatings
Anodic Polarization

The anodic polarization behavior of C_0, C_1, C_3 and C_5 coatings were examined using 3.5% NaCl solution in the potential range -1.3 to -0.4 V. The anodic polarization profiles of all coatings are shown in Fig. 1 (inset in the Fig. 1 shows the polarization curves in the potential range -1.3 to -0.4 V). The curve C_0 in Fig. 1 represents the polarization behavior of bare zinc coating, where as C_1, C_3 and C_5 represents the polarization behavior of zinc-TiO$_2$ composite coatings generated from bath solutions (Table 1) containing 1, 3 and 5 gL^{-1} of Degussa TiO$_2$. All composite coatings C_1, C_3 and C_5 showed higher corrosion potential with respect to C_0.
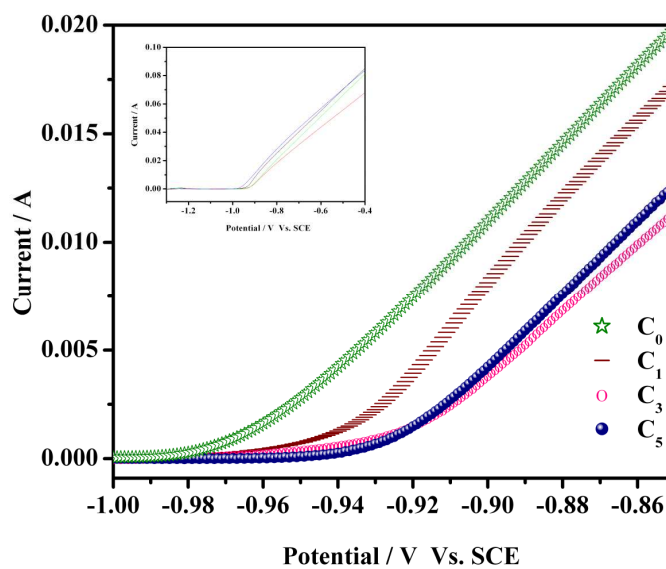

Fig. 1. Anodic polarization behavior for Zn C$_0$ and Zn-TiO$_2$ composite coatings C$_1$, C$_3$ and C$_5$

This shift of potential towards positive direction indicates the noble character of zinc-TiO$_2$ composite coating than bare zinc coating. The shift of potential further indicated high energy requirement for the dissolution of zinc from zinc-TiO$_2$ composite coating. Hence in zinc-TiO$_2$ composite coatings the reinforced TiO$_2$ nanoparticles retard the oxidation reaction given below

. $Zn \rightarrow Zn^{2+} + 2e^-$

Therefore, the anodic polarization results revealed that the anodic activity of composite coating is smaller than pure zinc coating.

Potentiodynamic polarization behavior of zinc and zinc-TiO$_2$ composite coatings
The anodic polarization profiles inferred the material corrosion behavior in aggressive media and gives either anodic or oxidation tendency of the material. The Tafel plots used to quantify the polarization results and corrosion rate was obtained.

The potentiodynamic polarization experiments were carried out in 3.5% NaCl solution. The working electrode was either of bare zinc coating C_0 or any one of the composite coatings C_1 or C_3 or C_5. All polarization results were measured at open circuit potential (OCP) of respective coatings C_0, C_1, C_3 and C_5. The Tafel parameters and other electro kinetic parameters of coatings are listed in Table 2.

The Tafel plots of all coatings are shown in Fig. 2. According to Table 2 the corrosion potential values of composite coatings were considerably positive when compare to that of C_0 coating. Also the corrosion current and corrosion rate of the composite coatings is minimum than that of pure zinc coating. These observation evidences the noble character of zinc-TiO$_2$ composite. The corrosion resistance property of coatings were in the order $C_0<C_1<C_5<C_3$. This reveal that the composite coating C_3 (coating obtained from the plating bath containing 3 gL^{-1} of Degussa TiO$_2$

_____

nanoparticles) is more corrosion resistant than other coatings. However, all the composite coatings are stable towards external aggressive media when compare to pure zinc coating.

Table-2: Electrochemical parameters estimated from potentiodynamic polarization curves

Specimen	E_{corr} in V	I_{corr} in $\mu A \, cm^{-2}$	β_a in mv dec^{-1}	β_c in mv dec^{-1}	Corrosion rate $\mu g \, hr^{-1}$
C_0	-1.055	6.203	46.29	320.82	7.332
C_1	-1.037	5.403	30.13	177.02	6.389
C_3	-1.027	2.749	44.64	192.38	3.251
C_5	-1.031	3.323	27.85	289.68	3.930

The deposits obtained with TiO_2 nanoparticles loaded plating bath showed corrosion resistance towards external aggressive media. The corrosion resistance of zinc-TiO_2 composite coatings can be described by the following factors. The co-deposited TiO_2 nanoparticles minimized the defects which act as active sites for corrosion; on the other hand, the uniformly distributed TiO_2 nanoparticles in the deposit behave as passive layer between corrosive media and deposit surface.
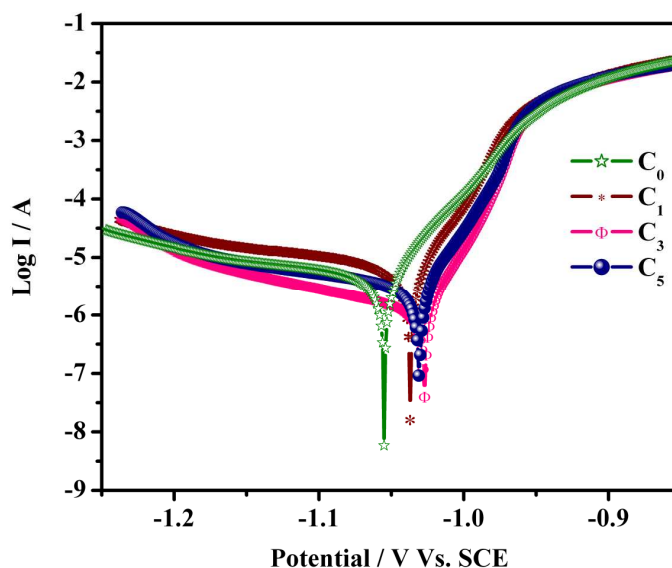

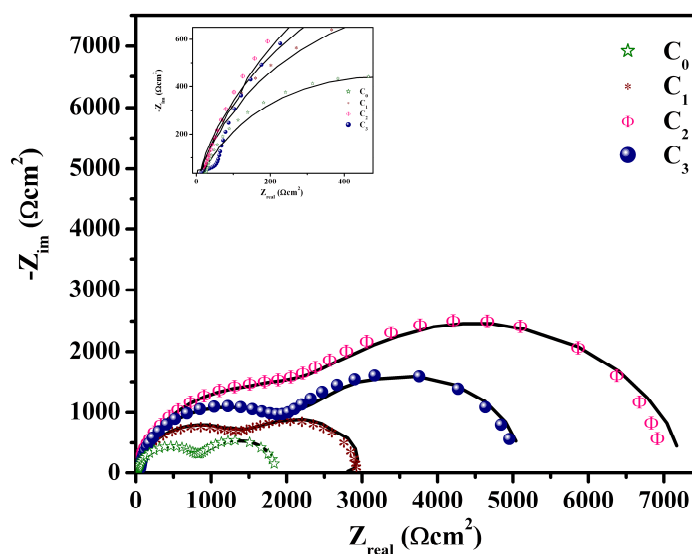**Fig. 2. Potentiodynamic polarization curves for coatings C_0, C_1, C_3 and C_5 in 3.5%NaCl solution**

Fig. 3. Experimental (――――) and simulated (symbol) Nyquist plots of Zn coating C_0, Zn-TiO_2 composite coatings C_1 and C_2 in 3.5% NaCl

_____

Electrochemical impedance studies

EIS data were displayed as typical Nyquist plots (Z_{re} / Z_{img}). The impedance plots corresponds to pure zinc coating C_0 and zinc-TiO$_2$ coatings C_1, C_3 and C_5 immersed in non-deaerated 3.5% NaCl solution measured at the frequency range 0.1 Hz to 10 kHz are shown in Fig. 3. The impedance measurements were carried out at OCP of the corresponding coatings. The analysis of shape of the impedance spectra help to understand the electrochemical process occurring at the surface. The Nyquist plots in Fig. 3 shows three capacitive loops or three time constants are present in higher, middle and lower frequency range. The resolved high frequency capacitive loop is presented as insert in corresponding Nyquist plot.

A more detailed analysis of impedance spectra was performed by fitting the measured EIS plots with electrical equivalent circuit (EEC). This means that obtaining a good fit does not imply that the used model is correct. Because the shape of the spectra is influenced by the electrochemical process at the surface and/or by the geometric factors of the electrode [20].

However, in the present work the experimental data were fitted with an electrical (3 RC) equivalent circuit Fig. 4 using ZSimpWin 3.21 Software.

In this circuit, each element is attributed to the following contributions [21, 22, 23 and 24].

R_e: is the electrolyte resistance appeared between the reference electrode and the surface of the coated specimen. i.e., working electrode.

The high frequency contribution (C_f - R_f) is ascribed to the dielectric character of the thin surface layer formed from the corrosion products (C_f) and its electrical leakage from ionic conduction through its pores (R_f).

The medium frequency contribution is attributed to the double layer capacitance (C_{dl}) at the electrolyte / coated surface (zinc and zinc-TiO$_2$) interface at the bottom of the pores coupled with the charge transfer resistance (R_{ct}). This charge transfer resistance is closely related to corrosion rate.

The low frequency couples (C_F - R_F) may related to a redox process taking place at the surface likely involving the thin layer of corrosion products accumulated at the electrolyte / working electrode surface interface.
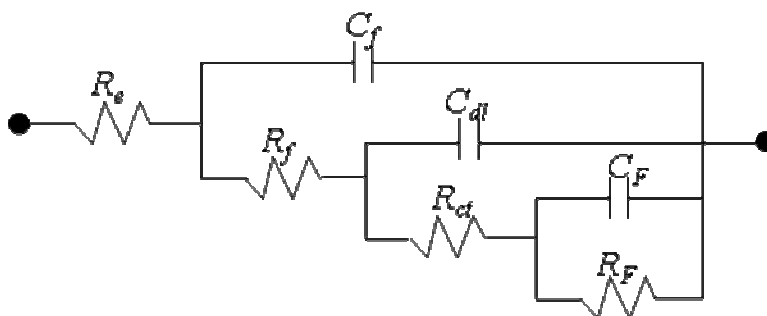

Fig. 4. Electrical equivalent circuit used for simulation of EIS data of Zn and Zn-TiO$_2$ coatings

The calculated impedance data from the equivalent circuit approaches the experimental data corresponds to the zinc coatings obtained in the absence and in the presence of TiO$_2$. The Table 3 gives the values of impedance elements obtained by EEC modeling of experimental data.

Table-3: Corrosion parameters calculated from (3RC) EEC simulated EIS measurements

Specimen	C_f in μF cm^{-2}	R_f in Ω cm^2	C_{dl} in μF cm^{-2}	R_{ct} in Ω cm^2	C_F in μF cm^{-2}	R_F in Ω cm^2	*R_p in kΩ cm^2
C_0	1.623	63.39	5.407	853.9	177.2	950.8	1.868
C_1	1.473	99.65	2.699	1498	58.28	1352	2.949
C_3	1.192	111.7	2.325	2649	25.03	4165	6.925
C_5	0.9104	123.8	3.53	2144	68.36	2803	5.070

(*R_p = R_f + R_{ct} + R_F)

Deposits obtained from all the concentration of TiO$_2$ particles acquires larger R_f values with lower C_f values, it may due to the formation of thin uniform layer of corrosion products on zinc-TiO$_2$ coatings and this layer resists the ionic conduction through the pores when compare to zinc deposit. However, the TiO$_2$ reinforced zinc deposits persists

higher charge transfer resistance value along with decrease in double layer capacitance value compare to zinc deposit. The decrease in C_{dl} value is attributed to a decrease in active sites because of the occluded TiO_2 nanoparticles. The contrast in the R_F and C_F values confirms the growth of the corrosion product layer during the measurements.

The polarization resistance (R_p) values were calculated by adding R_f, R_{ct} and R_F resistance values. The composite coatings C_1, C_3 and C_5 posses higher R_p values than C_0. Among these C_3 (3 gL^{-1} TiO_2) shows highest Rp value but lower values in the case of C_1 and C_5 than C_3, may be due to heterogeneities produced from the incorporated TiO_2 particles. Hence 3 gL^{-1} TiO_2 concentration was selected as optimum particle concentration. Finally it reveals that zinc coating obtained in presence of TiO_2 particles in the bath posses higher corrosion resistance property than the zinc coating obtained in absence of these particles.

The gathered results reveal that zinc-TiO_2 composite coatings are more stable towards external aggressive media when compare to pure zinc coating. It may due to influence of TiO_2 nanoparticles on the morphology and microstructure of zinc deposit. Hence the coatings C_0 and C_3 were characterized in order to know the effect of TiO_2 nanoparticles on morphology and microstructure of composite coatings.

Surface characterization

The presence of TiO_2 nanoparticles in composite coating was confirmed from the EDX spectra analysis of the deposit C_3 and is shown in Fig. 5. The peak corresponds to Ti and O in the EDX spectra confirmed the inclusion of TiO_2 nanoparticles in zinc matrix during deposition process. And 0.64 %of Ti content was observed for C_3 deposit. The SEM images of C_0 and C_3 were recorded and given in Fig. 6. Both images showed similar shape of randomly oriented hexagonal platelets. And the firmly bound TiO_2 nanoparticles were observed on the surface of composite coating. However, C_3 showed smaller, uniform grains with more compact crystallites than C_0.
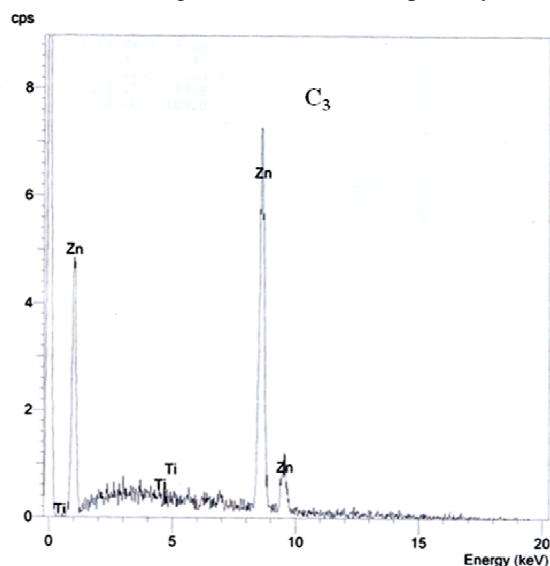

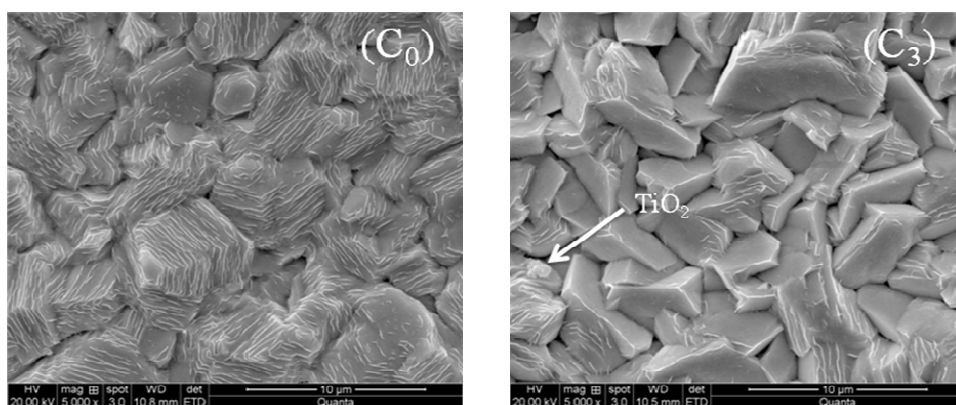**Fig. 5. EDX spectra of composite coating C_3**

Fig. 6. SEM surface morphology of coatings C_0 and C_3

This indicated that the TiO_2 particles were incorporated in the zinc matrix of the composite coating. So the incorporated TiO_2 particles offers more surface area for nucleation, thus the number of nucleation sites increases with decreasing the rate of crystal growth. This refines the grain size and renders the composite with compact arrangement [25]. Also, the pits observed on the surface of pure zinc coating were minimized in composite coating. Because the embedded TiO_2 nanoparticles minimized these gaps by entering into them while electrodeposition and brings the compact nature to the deposit.

The XRD patterns of the deposits C_0 and C_3 are given in Fig. 7. XRD graph confirms that the intensity of diffraction lines of C_3 decreased with larger width when compare to pure zinc coating. Further the average crystal size of two deposits, as plated zinc C_0 and zinc-TiO_2 composite C_3 was calculated from Scherer equation. The average crystal size of C_0 is   83 nm and that of C_3 is 61 nm. This inferred that the inclusion of TiO_2 brings down the crystal size of coating. This result is supported by SEM images Fig. 6.

$$L = \frac{K\lambda}{\beta\, cos\ \theta}$$

K-Scherer constant; λ-Wavelength of scattering; β-Full width half maxima, θ-Scattering angle; L-Average crystal size.
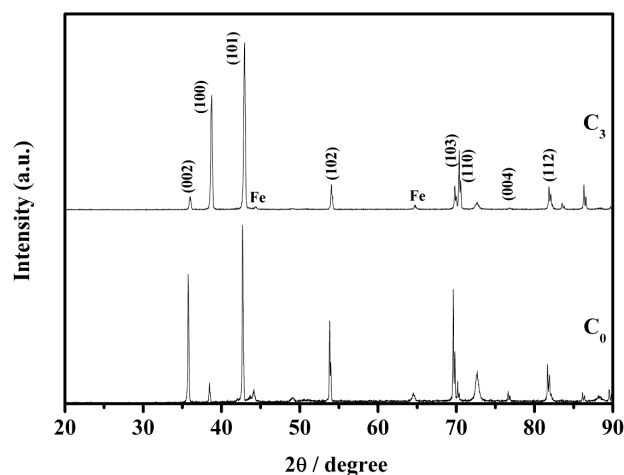

Fig. 7. XRD patterns of Zn coating (C_0) and Zn-TiO_2 (C_3) coating

The characteristic peak of TiO_2 in composite coating was not observed in the XRD patterns maybe due to the little content (0.64% ≡ EDS) in composite coatings. However, the EDS analysis confirmed the existence of TiO_2 particles in composite coating.

The TiO_2 is a second phase particle, initially present in the plating bath and then included in the deposit changes latter's properties which influence its corrosion behavior. These TiO_2 particles, after inclusion, change the smoothness, porosity, appearance of the coating and also produce stresses, generate defects and disorder the crystallographic structure. The solid particles influences the crystallization process, they disturb the regular growth of zinc crystals and creates new nucleation sites. To know the growth of new crystal plane after the inclusion of TiO_2 in zinc deposit the texture co-efficient (Fig. 8) was calculated for each peaks of diffraction patterns of both C_0 and C_3 coatings.

The texture co-efficient (Tc) can be calculated by using the equation Tc = [I(hkl)/∑(I(hkl)] × [∑IO(hkl)/IO(hkl)] [18]. Where $I_{(hkl)}$ is the peak intensity of electrodeposits and ∑I(hkl) is the sum of intensities of the independent peaks. And 'O' refers to the standard zinc powder sample. The determined texture co-efficient are plotted in Fig. 8. In bare zinc coating the majority of the zinc crystallites are oriented parallel to the (0 0 2) and (0 0 4) planes. But in the case of zinc-TiO_2 composite coating (C_3) the preferential orientation changes to (1 0 0) and (1 1 0). Therefore it suggests that the incorporated TiO_2 particle in zinc matrix changes the preferred orientation of zinc crystallites.
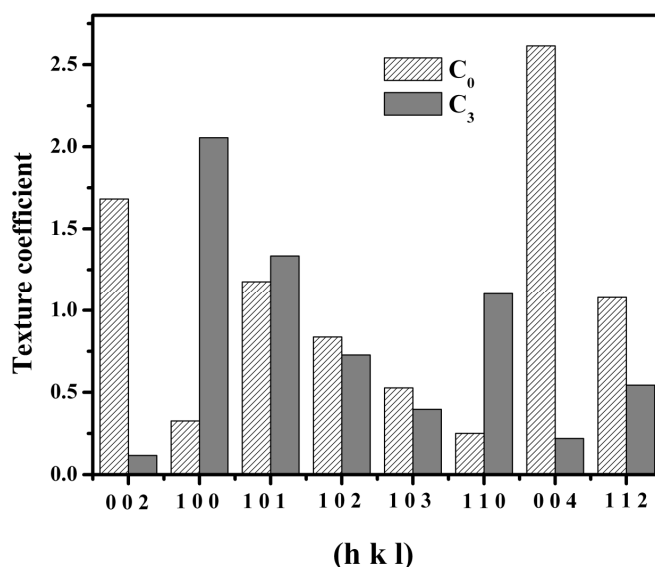
Fig. 8. Preferential orientation of Zn films in C_0 and C_3.

CONCLUSION

The zinc and zinc-TiO_2 composite coating were generated from the plating bath given in Table 1. The composite coating obtained from optimized bath containing 3 g L^{-1} of TiO_2 showed good corrosion resistance property compare to other coatings produced from solutions having different amount of TiO_2. The results of Tafel plots and impedance were matching with each other. The study confirms the optimization of particles amount in the bath is needed and they also responsible for improving corrosion resistance property of zinc coating. The TiO_2 particles changed the preferred orientation of crystal of zinc during deposition and it is included in the deposit giving zinc-TiO_2 composite coating. The morphology and microstructural change in composite coatings lead to exhibit better corrosion resistance property compare to pure zinc coating.

REFERENCES

[1] CB Wang; DL Wang; WX Chen; YY Wang. *Wear.*, **2002**, 253, 563-571.
[2] BM Praveen; TV Venkatesha. *Appl. Surf. Sci.,* **2008**, 254, 2418-2424.
[3] Maria Lekka; Niki Kouloumbi; Mauro Gajo; Pier Luigi Bonora. *Electrochim. Acta.,* **2005**, 50, 4551- 4556.
[4] Wei Wang; Feng-Yan Hou; Hui Wang; He-Tong Guo. *Scr. Mater.,* **2005**, 53, 613-618.
[5] S Harsha; DK Dwived; A Agarwal. *J. Mater. Eng. Perform.,* **2008**, 17, 104-110.
[6] Gang Wu; Ning Li; Derui Zhou; Kurachi Mitsuo. *Surf. Coat. Technol.,* **2004**, 176, 157-164.
[7] JN Balaraju; Kalavati; K.S. Rajam. *Surf. Coat. Technol.,* **2006**, 200, 3933-3941.
[8] G Heidari; H Tavakoli; SM Mousavi Khoie. *J. Mater. Eng. Perform.,* **2010**, 19, 1183–1188.
[9] BM Praveen; TV Venkatesha. *J. Alloys. Compd.,* **2009**, 482, 53-57.
[10] Beekanahalli Mokshanatha Praveen; Thimmappa Venkatarangaiah Venkatesha; Yanjerappa Arthoba Naik; Kalappa Prashantha. *Synth. React. Inorg. Met-Org. Chem.,* **2007**, 37, 461-465.
[11] HB Muralidhara; J Balasubramanyam; Y Arthoba Naik; K Yogesh Kumar; H Hanumanthappa; MS Veena. *J. Chem. Pharm. Res.,* **2012,** 4, 6871-6880.
[12] M Azizi; W Schneider; W Plieth. *J. Solid. State. Electrochem.,* **2005**, 9, 429-437.
[13] Dinghan Xiang; Kunlun Shan. *Wear.,* **2006**, 260, 1112-1118.
[14] SMA Shibli; VS Dilimon; Smitha P Antony; R Manu. *Surf. Coat. Technol.,* **2006**, 200, 4791-4796.
[15] Lawrence W Miller; M. Isabel Tejedor-Tejoder; Marc A Anderson. *Environ. Sci.Technol.,* **1999**, 33, 2070-2075.
[16] Bo Sun; Ettireddy P Reddy; Panagiotis G Smirniotis. *Environ. Sci. Technol.,* **2005**, 39, 6251-6259.
[17] Amy L Linsebigler; Guangquan Lu; John T Yates. Jr. *Chem. Rev.,* **1995**, 95, 735-758.
[18] J Fustes; A Gomes; MI da Silva Pereira. *J. Solid. State. Electrochem.,* **2008**, 12, 1435-1443.

[19] GM Treacy; GD Wilcox; MOW Richardson. *Surf. Coat. Technol.,* **1999**, 114, 260-268.

[20] Fabio La Mantia; Jens Vetter; Petr Novak. *Electrochim. Acta.,* **2008**, 53, 4109-4121.

[21] L Muresan; S Varavara; E Stupnisek-Lisac; H Otmacic; K Marusic; S Horvat-Kurbegovic; L Robbiola; K Rahmouni; H Takenouti. *Electrochim. Acta.,* **2007**, 52, 7770-7779.

[22] A Dermaj; N Hajjaji; S Joiret; K Rahmouni; A Srhiri; H Takenouti; V Vivier. *Electrochim. Acta.,* **2007**, 52, 4654-4662.

[23] PJ Kinlen; DC Silverman; CR Jeffreys. *Synth. Met.,* **1997**, 85, 1327-1332.

[24] Adriana Vlasa; Simona Varvara; Aurel Pop; Caius Bulea; Liana Maria Muresan. *J. Appl. Electrochem.,* **2010**, 40, 1519-1527.

[25] Lei Shi; Chufeng Sun; Ping Gao; Feng Zhou; Weimin Liu. *Appl. Surf. Sci.,* **2006**, 252, 3591-3599.